

# Radiative Transfer Code SHARM for Atmospheric and Terrestrial Applications

**A. I. Lyapustin**

University of Maryland Baltimore County GEST, NASA Goddard Space Flight Center, Greenbelt, Maryland.

**Abstract.** This paper gives an overview of the radiative transfer code SHARM based on the method of spherical harmonics. Being as rigorous and accurate as DISORT, code SHARM offers advantages in the speed of calculations and user convenience. It handles multiple wavelengths in one run and performs simultaneous calculations for different solar zenith angles (SZA), view zenith angles (VZA) and view azimuths. The Rayleigh scattering is automatically included as a function of wavelength, surface elevation and selected vertical profile of one of the standard atmospheric models. The Delta-M method is implemented for calculations with highly anisotropic phase functions. SHARM has several built-in models of the land and wind-ruffled water surface bi-directional reflectance that are most widely used in the research and satellite data processing. The paper also describes a modification of code SHARM with the built-in Mie algorithm designed for calculations with spherical aerosols.

## 1. Introduction

In the past several years we have witnessed a dramatic expansion of knowledge on our living environment coming from operational ground based and space-borne remote sensing systems. For example, MODIS<sup>1-2</sup> and MISR<sup>3</sup> are instruments of a new generation conducting global operational monitoring of a large number of atmospheric and surface parameters from space. The ground-based Aerosol Robotic Network<sup>4</sup> (AERONET) provides characterization of atmospheric column aerosol and water vapor for more than 170 locations worldwide. These and other sources of information dramatically enhance our capabilities to accurately model solar radiative transfer in the Earth-atmosphere system, and improve our understanding of the radiative budget and climate forcing factors of our planet. Such a research needs rigorous, fast and user convenient radiative transfer (RT) codes that can be directly used with the aerosol and surface reflectance models and data types available from the operational networks and space borne global observing systems.

Presently there are several publicly available RT codes for the atmospheric and land remote sensing communities: the most broadly used are 1D codes DISORT<sup>5</sup> and 6S<sup>6</sup>, and 3D code SHDOM<sup>7</sup>. We are presenting a new version of code SHARM<sup>8-9</sup> that implements method of spherical harmonics (MSH). Being as rigorous and accurate as DISORT, code SHARM offers advantages in speed of calculations and user convenience. This paper describes the latest version of SHARM upgraded with Delta-M<sup>10</sup> method, and a modification of code combined with MIE algorithm (SHARM-Mie) that is particularly convenient for the multi-wavelength calculations with spherical aerosols. Another code SHARM-3D designed for 3D calculations over inhomogeneous surfaces is described in the companion paper<sup>11</sup>.

## 2. Overview

Code SHARM solves the monochromatic unpolarized plane-parallel 1D problem with vertically non-uniform atmosphere and several broadly used models of land/ocean surface bi-directional reflectance factor (BRF). It calculates radiance and fluxes at the interfaces of atmospheric layers. When the surface is Lambertian, it also calculates the path radiance, upward atmospheric transmittance, and spherical albedo of the atmosphere. SHARM handles multiple wavelengths in one run, and performs simultaneous calculations for different solar zenith angles (SZA), view zenith angles (VZA), and view

azimuths. The molecular scattering is added automatically according to the wavelength, surface height above the sea level, and selected atmospheric profile. The details of MSH algorithm along with the built-in models are given in the Appendix.

The code comes in package with program *Phase* that computes Legendre expansion coefficients of aerosol/cloud phase function ( $\chi(\gamma)$ ), and automatically normalizes it. *Phase* uses rational spline interpolation to compute  $\chi(\gamma)$  in the quadrature angles required for Legendre expansion, and in the arbitrary directions for the single scattering calculations. The rational spline provides an accurate smooth interpolation for the most anisotropic phase functions, where the conventional cubic spline often develops an oscillating error. The current version of *Phase* calculates up to 2000 non-zero Legendre coefficients using the high order Lobatto quadrature.

The input data are arranged in three files:

*Configuration file* (config.par) defines wavelengths, the order of MSH, the incidence-view geometry, the file names of input atmospheric and surface properties, and governs printing of the results. *Atmospheric Properties file* describes the model of atmosphere, and optical properties of aerosols or clouds. In code SHARM, the input includes optical thickness ( $\Delta\tau$ ), single scattering albedo ( $\omega$ ), and scattering function for each atmospheric layer. The atmospheric gaseous absorption is not automatically included in this version, and should be specified by the user if needed. *Surface Properties file* describes the model and parameters of surface reflectance. The details on parameters and input format are documented in “SHARM Manual”.

Another code SHARM-Mie is an integrated package that combines Mie calculations for the wavelengths of interest, automatic Legendre expansion of phase functions, and RT calculations with code SHARM. Aerosols are represented by polydisperse spherical particles with bi-modal lognormal size distribution or generic-form size distribution. The aerosol properties are assumed to be constant with altitude but the aerosol concentration can vary according to the specified vertical profile. Because the Mie calculations carry the main computational load, this approach is chosen to keep the computing time relatively low. On the other hand, the resulting atmospheric model is quite realistic and well suitable for the remote sensing studies of atmospheric aerosol and surface reflectance. The monodisperse Mie calculations are performed by the code *MIEnoP* of W. Wiscombe<sup>12</sup> translated into C language. The integration over size distribution is performed using Simpson’s quadrature with 2001 points. The integration limits are either given by the *min* and *max* radii of the generic-form size distribution, or set to  $r_{\min}=0.05 \mu\text{m}$  and  $r_{\max}=15 \mu\text{m}$  for the bi-modal distribution. The input differs from code SHARM in the file of *Atmospheric Properties*. Instead of optical parameters  $\{\Delta\tau, \omega, \chi(\gamma)\}$ , the user should specify relative vertical profile of aerosol and its microphysical properties, namely spectral index of refraction and particle size distribution.

The mentioned codes share a common library of files and are written in C language with C++ features.

### 3. Built-in Models

#### 3.1 Geometric Model

SHARM uses plane-parallel model of the atmosphere divided into  $K$  homogeneous layers. Each layer  $k$  is characterized by its optical thickness  $\Delta\tau_k = \tau_k - \tau_{k-1}$ , single scattering albedo  $\omega_k$ , and scattering function  $\chi_k(\gamma)$ . The total optical thickness and atmospheric layers are counted from the top of the atmosphere (TOA). In opposite, the altitude of interfaces ( $h_i$ ) is counted from the ground level, in agreement with the standard atmospheric profiles of temperature and pressure.

In the accepted coordinate system, solar zenith angle  $\theta_0$  (SZA) changes from 0 to 90°, and view zenith angle  $\theta$  (VZA) changes in the ranges 90-180° ( $\mu = \cos\theta < 0$ ) for upward directions (view geometry from space), and 0-90° ( $\mu > 0$ ) for downward directions (ground-based observations of sky radiance). The relative azimuth is calculated clockwise from the principal plane: it is defined so that  $\varphi = 0^\circ$  for the forward scattering, and  $\varphi = 180^\circ$  for the back-scattering direction.

### 3.2 Rayleigh Scattering

The scattering function of air is considered to be purely Rayleigh. It does not account for a slight asymmetry caused by depolarization. The vertical profile of molecular optical thickness is calculated as:

$$\tau^m(\lambda, z) = \int_0^z \sigma(\lambda, z') N(z') dz',$$

where  $\sigma$  is a Rayleigh scattering cross section per molecule,  $N(z) = N_s \frac{P(z)}{P_s} \frac{T_s}{T(z)}$  is a concentration of air molecules at altitude  $z$ , and  $P_s = 1013.25 \text{ mb}$ ,  $T_s = 273.15 \text{ K}$  are the standard pressure and temperature. The vertical profile of pressure and temperature can be selected from six standard atmospheric profiles<sup>13</sup> (Tropical, Midlatitude Summer, Midlatitude Winter, SubArctic Summer, SubArctic Winter, 1976 US Standard). The integral over altitude is evaluated with the gaussian quadrature.

The Rayleigh scattering cross section is calculated with the algorithm of Bodhain et al.<sup>14</sup>, which has a uniformly high accuracy across the spectral range from UV to the shortwave IR.

### 3.3 Surface BRF Models

Three broadly recognized BRF models of land surface reflectance are built in code SHARM (SHARM-Mie): Rahman-Pinty-Verstraete (RPV)<sup>15</sup> model, modified RPV (MRPV)<sup>16</sup> model, and a Li Sparse – Ross Thick reciprocal (LSRT)<sup>17</sup> model. The LSRT and MRPV models are used in the operational land reflectance algorithms of MODIS and MISR, respectively. All of these models are reciprocal and rotationally invariant, i.e. they depend only on relative azimuth, and are described by three parameters.

The ocean surface reflectance can be modeled with either azimuthally-independent model of Nakajima and Tanaka<sup>18</sup> (NT), or with the Cox and Munk<sup>19</sup> model with Grams-Charlier expansion (CM). Both models include bi-directional wave-shadowing factor of Nakajima and Tanaka<sup>18</sup>. The NT model depends only on the wind speed, whereas CM model additionally depends on the wind direction. The details of surface BRF models are given in Appendix B.

## 4. Accuracy and Convergence

Code SHARM was extensively validated<sup>8,20</sup> against code DISORT and also indirectly tested in the atmospheric correction of airborne measurements, e.g., over the dark ocean<sup>21</sup>. The most important parameter that controls the accuracy of solution is the order of MSH (parameter  $nb$ ) specified by the user. In essence, exactly  $nb$  coefficients of phase function are used in the multiple scattering calculations. The single-scattered radiance in SHARM is calculated using an exact formula and does not depend on  $nb$ . The solution for the multiple scattering converges to the true one at the increase of  $nb$ , however the computing time also grows approximately as  $nb^3$ .

Generally, the more asymmetric phase function, the higher  $nb$  is required to achieve a given accuracy. For typical continental/marine aerosols, the relative accuracy of 0.2-0.3% is achieved at  $nb=24-36$  in radiance calculations for the range of view/solar zenith angles up to 75-80°. The value of

$nb=128$  ensures the accuracy of  $\approx 0.02\%$ <sup>20</sup>. Generally, the convergence slows with the increase of zenith angle. Therefore, the higher orders  $nb$  should be used for high solar or view zenith angles to achieve the same relative accuracy.

For calculations with strongly asymmetric phase functions typical of clouds, with large forward scattering peak, even high orders of MSH may be insufficient. For these cases, we implemented the Delta-M method<sup>10</sup> that achieves the accuracy of about 1% at relatively low orders of MSH,  $nb=32-64$ , except for the aureole region and some transitional area around it (see also study<sup>22</sup>). As an example, Figure 1 shows a convergence of SHARM with and without Delta-M method for the case of cirrus cloud over anisotropic surface.

The above discussion on the accuracy and convergence pertains to the radiance calculations (specific intensity). Flux calculations require considerably smaller orders of MSH. For example, fluxes at  $nb=12-24$  are typically accurate to the fourth significant digit.

At typical orders of MSH ( $nb=24-48$ ), the runtime of code SHARM-Mie is almost entirely defined by Mie calculations. In order to minimize the runtime, only  $nb$  required coefficients of Legendre expansion are calculated each time.

## Conclusion

This paper gave an overview of code SHARM (SHARM-Mie) which is a rigorous yet rather fast code compared to other similar codes. SHARM is user-friendly due to built-in models of Rayleigh scattering and land/water surface reflectance, and its capability to perform simultaneous calculations for different illumination-view geometries as well as for the multiple wavelengths in one run. Currently we are integrating code SHARM with the Interpolation and Profile Correction (IPC) method<sup>23</sup> that will automatically include atmospheric gaseous absorption and will allow calculations with an arbitrary spectral resolution, from monochromatic to the shortwave broadband. The current version of code SHARM (SHARM-Mie, SHARM-3D) is available for public use via <ftp://ltpftp.gsfc.nasa.gov/projects/asrvn/>.

## APPENDIX

### A. Method of Spherical Harmonics

The diffuse radiance  $I(\tau; \mu, \varphi)$  is a solution to the following boundary-value problem:

$$\mu \frac{\partial I(\tau, \mu, \varphi)}{\partial \tau} + I(\tau, \mu, \varphi) = \frac{\omega}{4\pi} \int_0^{2\pi} d\varphi' \int_{-1}^1 \chi(\tau, \gamma) I(\tau, \mu', \varphi') d\mu' + S_\lambda \frac{\omega}{4} \chi(\tau, \gamma_0) \exp\left(-\frac{\tau}{\mu_0}\right) \quad (1a)$$

$$I(0; \mu, \varphi) = 0, \mu > 0$$

$$I(\tau_0, \mu, \varphi) = S_\lambda \mu_0 \rho(\mu_0, \mu, \varphi - \varphi_0) e^{-\tau_0/\mu_0} + \frac{1}{\pi} \int_0^{2\pi} d\varphi' \int_0^1 \rho(\mu', \mu, \varphi - \varphi') I(\tau_0, \mu', \varphi') \mu' d\mu', \mu < 0 \quad (1b)$$

Here,  $\rho$  is surface BRDF (unitless), and  $\pi S_\lambda$  is extraterrestrial spectral solar irradiance. The scattering function is normalized to unity,  $\frac{1}{2} \int_0^\pi \chi(\gamma) \sin \gamma d\gamma = 1$ .

To solve problem (1), the scattering function is expanded into Legendre polynomial series  $x(\gamma) = \sum_{n=0}^L \chi_n P_n(\cos \gamma)$ , with coefficients  $\chi_k = \frac{2k+1}{2} \int_{-1}^1 \chi(y) P_k(y) dy$ . Parameter  $L=nb$ , the order of MSH, defines the accuracy of expansion and of the solution for multiple scattering.

The application of an addition theorem for Legendre polynomials, and expansion of radiance into spherical harmonics transforms integro-differential equation (1) into the system of linear differential equations

$$A^m \frac{d\bar{\varphi}^m(\tau)}{d\tau} + C^m \bar{\varphi}^m(\tau) = e^{-\tau/\mu_0} \bar{f}^m(\tau). \quad (2)$$

Here  $\bar{\varphi}^m(\tau) = \{\varphi_m^m(\tau), \varphi_{m+1}^m(\tau), \dots, \varphi_{L_m}^m(\tau)\}^T$  is the vector of moments for  $m$ th azimuthal harmonic of radiance  $I^m(\tau, \mu)$ ,

$$I(\tau; \mu, \varphi) = \sum_{m=0}^{\infty} (2 - \delta_{0,m}) I^m(\tau, \mu) \cos m\varphi, \quad I^m(\tau, \mu) = \sum_{k=m}^{L_m} \frac{2k+1}{2} \varphi_k^m(\tau) Y_k^m(\mu). \quad (3)$$

In (3),  $Y_k^m(\mu) = \sqrt{\frac{(k-m)!}{(k+m)!}} P_k^m(\mu)$  are the normalized associated Legendre polynomials. Explicit expressions for matrices  $A^m$  and  $C^m$  and vector  $\bar{f}^m$  can be found in *Karp et al.*<sup>24</sup>, *Muldashev et al.*<sup>8</sup>. We use triangular system of equations (2), and the order of MSH  $L_m - m + 1$  is even for all  $m$ .

The boundary conditions at the top and bottom of the atmosphere are expressed for  $m$ th azimuthal harmonic in the form of *Marshak* as follows<sup>25,9</sup>:

$$\bar{\varphi}_{od}^m(0) - G^m \bar{\varphi}_{ev}^m(0) = 0, \quad (4a)$$

$$(I - 2N_{od}^m) \bar{\varphi}_{od}^m(\tau_0) + (G^m - 2N_{ev}^m) \bar{\varphi}_{ev}^m(\tau_0) = 2S_0 e^{-\tau_0/\mu_0} \bar{Q}^m(\mu_0). \quad (4b)$$

$\bar{\varphi}_{od}^m$  and  $\bar{\varphi}_{ev}^m$  are vectors consisting of odd and even elements of vector  $\bar{\varphi}^m$ , and  $I$  is an identity matrix. Matrix  $G^m$  and a method for its calculation can be found in *Dave*<sup>25</sup>.  $N_{od}^m$  and  $N_{ev}^m$  are quadratic

matrices of the order of  $\frac{L_m - m + 1}{2}$ :

$$(N_{ev}^m)_{l,k} = (4k + 2m + 2\delta_m - 3) \int_0^1 \mu' Q_l^m(\mu') Y_{m+\delta_m+2k-2}^m(\mu') d\mu', \quad (5a)$$

$$(N_{od}^m)_{l,k} = (4k + 2m - 2\delta_m - 1) \int_0^1 \mu' Q_l^m(\mu') Y_{m-\delta_m+2k-1}^m(\mu') d\mu', \quad l, k = 1, 2, \dots, \frac{L_m - m + 1}{2}, \quad (5b)$$

where  $\delta_m=0$  if  $m$  is even, and  $\delta_m=1$  if  $m$  is odd. The elements of vector  $\bar{Q}^m(\mu')$  are calculated from azimuthal harmonics of BRF:

$$Q_l^m(\mu') = \int_{-1}^0 \rho^m(\mu', \mu) Y_{m-\delta_m+2l-1}^m(\mu) d\mu. \quad (5c)$$

Previously<sup>9</sup> we used analytical formulas to integrate equations (5). Our further research with the BRF models built in SHARM showed that the use of Gaussian quadrature allows faster integration with an automatic selection of the quadrature order ( $\approx \frac{nb}{2} + 10$ ).

## A.1 Solution for Radiance

Solving system (2), (4) for each  $m=0, 1, \dots$  for vectors  $\vec{\varphi}^m(\tau)$  allows to compute diffuse radiance on the next step by summing series (3). Harmonics  $I^m(\tau, \mu)$  rapidly decrease in magnitude with increasing  $m$ , which terminates azimuthal series at some  $M_0$ .

Method of solution is an analytical integration of Eq. (2) within each atmospheric layer where atmospheric optical properties are constant (and hence matrices  $A^m$ ,  $C^m$ , and vector  $\vec{f}^m$ ). The singular-value decomposition of matrix  $B^m=(C^m)^{-1}A^m$  rigorously transforms the system of linear differential equations into the system of linear algebraic equations in  $K$  atmospheric layers with a block matrix,<sup>24</sup> which is successfully solved by a generalized Gauss elimination method. Further, the solution is smoothed with the *correction function method*<sup>8</sup>, which compensates errors due to truncation of the system of MSH, and due to an approximate form of the boundary conditions. This smoothing method also calculates the single-scattered radiance exactly regardless of the order of approximation of MSH.

If surface is Lambertian, code SHARM separately computes atmospheric path radiance  $D$ , which is a solution with the black surface, surface irradiance  $\pi E_0(\mu_0)$ , upward atmospheric transmittance  $T(\mu)$  and spherical albedo of atmosphere  $c_0$ . The total radiance is found using a well-known formula of Chandrasekhar<sup>26</sup>,

$$I(\mu_0, \mu, \varphi) = D(\mu_0, \mu, \varphi) + q \frac{E_0(\mu_0)T(\mu)}{1 - qc_0}. \quad (6)$$

## A.2 Delta-M Method

With the growth of a particle size, the scattered light concentrates more and more in the narrow peak in the forward scattering direction. Accurate Legendre expansion of such functions requires literally thousands of terms. In these conditions, the convergence of solution with increase of the order of MSH is very slow, which explains why RT calculations for cloudy atmospheres have always been very challenging.

To accelerate calculations, different approximations were developed<sup>22</sup>. In code SHARM, we have implemented the Delta-M method<sup>10</sup>, which approximates the forward peak with  $\delta$ -function,

$$\chi(\gamma) = F2\delta(0) + (1 - F)\chi^*(\gamma), \quad (7)$$

where  $F$  is a fraction of forward scattering. Delta-M method automatically conserves the first  $N$  moments of expansion:

$$\chi_n = F(2n + 1) + (1 - F)\chi_n^*, \quad (8)$$

where  $F = \frac{\chi_N}{2N + 1}$ , and  $\chi_n^* = \frac{\chi_n - F(2n + 1)}{(1 - F)}$ . The substitution of phase function (7) into Eq. (1a) leads

to the modified problem

$$\mu \frac{\partial I}{\partial \tau^*} + I = \frac{\omega^*}{4\pi} \int_0^{2\pi} d\varphi' \int_{-1}^1 \chi^*(\tau^*, \gamma) I(\tau^*, \mu', \varphi') d\mu' + S_\lambda \frac{\omega^*}{4} \frac{\chi(\tau, \gamma_0)}{1 - F} \exp\left(-\frac{\tau^*(1 - \omega F)^{-1}}{\mu_0}\right) \quad (9)$$

with truncated phase function  $\chi^*(\gamma)$  and scaled optical thickness and single scattering albedo

$$\tau^* = \tau(1 - \omega F), \quad \omega^* = \omega \frac{(1 - F)}{(1 - \omega F)}. \quad (10)$$

The new equation has the same form as the original one, only with scaled parameters and modified single-scattering source function.

Figure 1 shows convergence of code SHARM with and without Delta-M method for calculations with the phase function of cirrus cloud with the particle modal diameter 10  $\mu\text{m}$ . The accurate result corresponds to the converged high order MSH solution ( $nb=512$ ). Except for the aureole region and transitional zone of about  $20^\circ$ , the low-order  $nb=32-48$  Delta-M solution has an accuracy of about 1-2%.

## B. Surface BRF Models

Because there are different definitions of angles in the literature, and even differences in the formulation of BRF models are not exceptions, we consider it worthwhile to give analytical expressions that are coded in SHARM. For convenience of notations, the cosine of zenith angle below is always positive, and the upward view directions will be indicated as  $(-\mu)$ .

### B.1 Land: RPV and MRPV models

The RPV model depends on three parameters ( $\rho_0, k, \alpha$ ):

$$\rho(\mu_0; -\mu; \varphi) = \rho_0 M(k) F(\alpha) H(\rho_0), \quad (\text{L-1})$$

$$M(k) = [\mu\mu_0(\mu + \mu_0)]^{k-1}, \quad F(\alpha) = \frac{1 - \alpha^2}{[1 - 2\alpha \cos \gamma + \alpha^2]^{3/2}}, \quad H(\rho_0) = \left\{1 + \frac{1 - \rho_0}{1 + G}\right\}, \quad (\text{L-2})$$

where  $\gamma$  is angle of scattering,

$$\cos \gamma = -\mu_0\mu + \sqrt{1 - \mu_0^2} \sqrt{1 - \mu^2} \cos(\varphi - \varphi_0), \quad (\text{L-3})$$

and

$$G = \sqrt{tg^2\theta_0 + tg^2\theta + 2tg\theta_0tg\theta \cos(\varphi - \varphi_0)}. \quad (\text{L-4})$$

Note that the hot spot lies in the direction of backscattering,  $\varphi - \varphi_0 = \pi$ .

Usually, the Minnaert's exponent  $k$  is less than 1. It means that at small values of  $\mu, \mu_0$ , the total BRF may become unphysically large, and surface albedo at high SZA may exceed 1. As a remedy, our algorithm sets the low limit of  $\mu, \mu_0$  in BRF calculations to 0.03. Although this approach is not rigorous, it provides stable solution for the common cases.

In the MRPV model, the term  $F(\alpha)$  is substituted by  $F(\alpha) = \exp(\alpha \times \cos \gamma)$ . This modification yields a nearly linear expression for the BRF model parameters after logarithmic transformation.

### B.2 Land: Linear LSRT model

This model is represented by a sum of Lambertian, geometric-optics and volume scattering terms:

$$\rho(\mu_0, -\mu, \varphi) = k_L + k_{go} f_{go}(\mu_0, \mu, \varphi) + k_v f_v(\mu_0, \mu, \varphi). \quad (\text{L-5})$$

The kernel functions are given by the following expressions:

$$f_v = \frac{(\frac{\pi}{2} - \gamma) \cos \gamma + \sin \gamma}{\mu_0 + \mu} - \frac{\pi}{4}, \quad (\text{L-6})$$

$$f_{go} = O(\mu_0, \mu, \varphi) - \mu'^{-1} - \mu_0'^{-1} + \frac{1}{2}(1 + \cos \gamma')\mu'^{-1}\mu_0'^{-1}, \quad (\text{L-7})$$

where

$$O(\mu_0, \mu, \varphi) = \frac{1}{\pi}(t - \sin t \cos t)(|\mu'|^{-1} + \mu_0'^{-1}), \quad (\text{L-8})$$

$$\cos t = \frac{h \sqrt{(G')^2 + (tg \theta'_0 tg \theta' \sin(\varphi - \varphi_0))^2}}{b \left( |\mu'|^{-1} + \mu_0'^{-1} \right)}, \text{ with a constraint } |\cos t| \leq 1. \quad (\text{L-9})$$

The primed angles  $(\theta'_0, \theta')$  are obtained by scaling  $tg \theta' = \frac{b}{r} tg \theta$ . Note that  $\cos \gamma'$  in (L-7) and  $G'$  in (L-9) are calculated for primed angles  $(\theta'_0, \theta')$  using equations (L-3) and (L-4), respectively.

The ratio of structural parameters is fixed<sup>17</sup> ( $h/b=2$  and  $b/r=1$ ). Thus, the functions  $f_v, f_{go}$  depend on angles only, and BRF is defined by three coefficients  $\{k_L, k_{go}, k_v\}$ .

It is important to keep in mind that the functions  $f_v, f_{go}$  take both positive and negative values. Our experience with processing MISR measurements<sup>27</sup> shows that the best-fit weights  $k_{go}$  and  $k_v$  for different landcover types are often negative, although the resulting BRF and surface albedo remain positive. For this reason, different terms of this model should only be considered as mathematical functions rather than physical components of the surface reflectance. Also, one needs to exercise caution with this model at high zenith angles larger than  $80^\circ$ , when the BRF may become negative or, in the contrary, grow very fast<sup>28</sup>.

### B.3 Ocean: Azimuthally-Independent Model of Nakajima and Tanaka (NT)

Following Nakajima and Tanaka<sup>18</sup>, the reflection coefficient is expressed as follows:

$$R(\mu', -\mu, \varphi - \varphi') = \frac{1}{4\mu\mu_n} R^{Fr}(\chi) P(\mu_n) S(\mu', \mu), \quad (\text{O-1})$$

where  $R^{Fr}$  is Fresnel reflectance for unpolarized radiance,  $P(\mu_n)$  is the probability density function of wave slope distribution, and  $S$  is the wave shadowing factor. The refractive index of water required to compute  $R^{Fr}$  is obtained by spline interpolation from spectral data of *Hale and Querry*<sup>29</sup>.

The probability density function of slope distribution is given by

$$P(\mu_n) = \frac{1}{\pi\sigma^2\mu_n^3} \exp\left(-\frac{1-\mu_n^2}{\sigma^2\mu_n^2}\right), \quad (\text{O-2})$$

where  $\sigma^2 = 0.00534u$ , and  $u$  [m/s] is wind speed 10 meters above the water surface. Following *Gordon and Wang*<sup>30</sup>,

$$\frac{1}{4\mu\mu_n} P(\mu_n) = \frac{a^2}{\mu\pi\sigma^2} \exp\left(\frac{1-2a}{\sigma^2}\right),$$

where  $a = \frac{1 + \cos 2\chi}{(\mu + \mu')^2}$ , and  $\cos 2\chi = \mu\mu' - \sqrt{1-\mu^2} \sqrt{1-\mu'^2} \cos(\varphi - \varphi')$ .

Finally, the wave-shadowing factor is written as:

$$S(\mu', \mu) = \frac{1}{1 + F(g) + F(g')}, \quad g = \frac{\mu}{\sigma\sqrt{1-\mu^2}},$$

where

$$F(g) = \frac{1}{2} \left[ \frac{\exp(-g^2)}{g\sqrt{\pi}} - \frac{2}{\sqrt{\pi}} \int_g^\infty \exp(-t^2) dt \right] = \frac{\exp(-g^2)}{2g\sqrt{\pi}} - \frac{1}{2} + \Phi(\sqrt{2}g),$$

$\Phi(\sqrt{2}g) = \frac{1}{\sqrt{2\pi}} \int_0^{\sqrt{2}g} \exp(-\frac{z^2}{2}) dz$  is the probability integral for the normal distribution.

For compliance with the general form of the boundary condition (1b), the BRF is written as:

$$\rho(\mu', -\mu, \varphi - \varphi') = \frac{\pi}{\mu'} R(\mu', -\mu, \varphi - \varphi').$$

#### B.4 Cox-Munk Model with Gram-Charlier Expansion (CoxMunk)

Let us consider the right-handed system of coordinates  $(X, Y, Z)$  centered in the observation point  $O$ . Vector  $OY$  lies in the principal plane and points in the opposite to the Sun direction, and vector  $OX$  is perpendicular to the principal plane. The wave slope (facet) has two components:

$$Z_x = \partial Z / \partial X = \sin \alpha \tan \beta = \frac{\sin \theta \sin \varphi}{\mu + \mu_0}, \quad Z_y = \partial Z / \partial Y = \cos \alpha \tan \beta = \frac{\sin \theta \cos \varphi - \sin \theta_0}{\mu + \mu_0}, \quad (\text{O-3})$$

where  $\alpha$  is the azimuth of ascent (clockwise from the sun), and  $\beta$  is the tilt.

If the distribution of the slope components depends on the wind direction, let us rotate the coordinate system about axis  $OZ$  by the angle  $\Delta\varphi_w = \varphi_{wind} - \varphi_0$  clockwise. This gives the new coordinate system  $(X', Y', Z')$ , where the axis  $OY'$  is aligned with the up-wind direction. In the new coordinates, the slopes (O-3) become:

$$Z_u = Z_{y'} = Z_y \cos \Delta\varphi_w + Z_x \sin \Delta\varphi_w, \quad Z_c = Z_{x'} = -Z_y \sin \Delta\varphi_w + Z_x \cos \Delta\varphi_w, \quad (\text{O-4})$$

and the slope probability density function can now be written as:

$$P(\mu_n) = \frac{1}{2\pi\sigma_u\sigma_c\mu_n^3} \exp\left\{-\frac{\xi^2 + \eta^2}{2}\right\} GC, \quad \eta = Z_u / \sigma_u, \quad \xi = Z_c / \sigma_c. \quad (\text{O-5})$$

The subscripts  $u$  and  $c$  refer to the up-wind and cross-wind components, and the term  $GC$  denotes Gram-Charlier expansion<sup>19</sup>.

In code SHARM, the diffuse reflected radiance is always computed with isotropic  $NT$  model, and the direct reflected radiance can be computed with either  $NT$  model or the described *CoxMunk* model. In the last case, the two models are linked by the ‘‘energy conservation’’ condition  $\sigma_u^2 + \sigma_c^2 = \sigma_{NT}^2 = 0.00534u$ . In the experiments, Cox and Munk observed the range of anisotropy  $\sigma_u / \sigma_c = 1-1.8$ , with an average value of 1.34. Currently, SHARM uses  $\sigma_u^2 = 0.6\sigma_{NT}^2$ ,  $\sigma_c^2 = 0.4\sigma_{NT}^2$ , so  $\sigma_u / \sigma_c = 1.5$ .

**Acknowledgement.** This work was supported by NASA EOS Science and NASA NPP grants.

## References

1. King, M. D., W. P. Menzel, Y. J. Kaufman, D. Tanre, B. C. Gao, S. Platnick, S. A. Ackerman, L. A. Remer, R. Pincus, and P. A. Hubanks, "Cloud and aerosol properties, precipitable water, and profiles of temperature and humidity from MODIS," *IEEE Trans. Geosci. Remote Sens.* **41**, 442-458 (2003).
2. Justice, C. O., J. R. G. Townshend, E. F. Vermote, E. Masuoka, R. E. Wolfe, N. Saleous, D. P. Roy, and J. T. Morisette, "An overview of MODIS Land data processing and product status," *Remote Sens. Environ.* **83**, 3-15, (2002).
3. D. J. Diner et al., "Multi-angle Imaging SpectroRadiometer (MISR) instrument description and experiment overview," *IEEE Trans. Geosci. Remote Sens.* **36**, 1072-1087 (1998).
4. Holben, B. N., T. F. Eck, I. Slutsker, D. Tanré, J. P. Buis, A. Setzer, E. Vermote, J. A. Reagan, Y. J. Kaufman, T. Nakajima, F. Lavenue, I. Jankowiak, A. Smirnov, "AERONET-A Federated Instrument Network and Data Archive for Aerosol Characterization," *Rem. Sens. Environ.* **66**, 1-16 (1998).
5. K. Stamnes, S. C. Tsay, W. Wiscombe, and K. Jayaweera, "Numerically stable algorithm for discrete-ordinate-method radiative transfer in multiple scattering and emitting layered media," *Appl. Opt.* **27**, 2502-2509 (1988).
6. E. F. Vermote, D. Tanre, J. L. Deuze, M. Herman, and J.-J. Mockette, "Second simulation of the satellite signal in the solar spectrum, 6S: An overview," *IEEE Trans. Geosci. Remote Sens.* **35**, 675-686 (1997).
7. K. F. Evans, "The spherical harmonics discrete ordinate method for three-dimensional atmospheric radiative transfer," *J. Atm. Sci.* **55**, 429-446 (1998).
8. Muldashev, T. Z., A. I. Lyapustin, and U. M. Sultangazin, Spherical harmonics method in the problem of radiative transfer in the atmosphere-surface system, *J. Quant. Spectrosc. Radiat. Transfer* **61**, 393-404 (1998).
9. A. I. Lyapustin and T. Z. Muldashev, "Generalization of Marshak boundary condition for non-Lambert reflection," *J. Quant. Spectrosc. Radiat. Transfer* **67**, 457-464 (2000).
10. Wiscombe W. J., "Delta-M Method - Rapid Yet Accurate Radiative Flux Calculations For Strongly Asymmetric Phase Functions," *J. Atmos. Sci.* **34**, 1408-1422 (1977).
11. A. Lyapustin, and Y. Wang, "Parameterized code SHARM-3D for Radiative Transfer over Inhomogeneous Surfaces." *This issue*.
12. Wiscombe, W., "Improved Mie scattering algorithms," *Appl. Opt.* **19**, 1505-1509 (1980).
13. F. X. Kneizys, L. W. Abreu, G. P. Anderson, J. H. Chetwynd, E. P. Shettle, A. Berk, L. S. Bernstein, D. C. Robertson, P. Acharya, L. S. Rothman, J. E. A. Selby, W. O. Gallery, S. A. Clough, "The MODTRAN 2/3 Report and LOWTRAN 7 Model," Modtran Report: Ontar Corporation, North Andover, MA, 261 pp. (1996).
14. B. A. Bodhaine, N. B. Wood, E. G. Dutton, J. R. Slusser, "On Rayleigh Optical Depth Calculations," *J. Atmos. Oceanic Technology* **16**, 1854-1861 (1999).
15. Rahman, H., B. Pinty, and M. M. Verstraete, "Coupled surface-atmosphere reflectance (CSAR) model. 2. Semiempirical surface model usable with NOAA advanced very high resolution radiometer data," *J. Geophys. Res.* **98**, 20,791-20,801 (1993).
16. Martonchik, J. V., D. J. Diner, B. Pinty, M. M. Verstratete, R. B. Myneni, Yu. Knyazikhin, and H. R. Gordon, "Determination of land and ocean reflective, radiative and biophysical properties using multiangle imaging," *IEEE Trans. Geosci. Remote Sens.* **36**, 1266-1281 (1998).
17. Lucht W., Schaaf C. B., Strahler A. H., "An algorithm for the retrieval of albedo from space using semiempirical BRDF models," *IEEE Trans. Geosci. Remote Sens.* **38**, 977-998 (2000).

18. Nakajima, T., and M. Tanaka, "Effect of wind-generated waves on the transfer of solar radiation in the atmosphere-ocean system," *J. Quant. Spectrosc. Radiat. Transfer* **29**, 521-537 (1983).
19. C. Cox and W. Munk, "Measurements of the roughness of the sea surface from photographs of the Sun's glitter," *J. Opt. Society Am.* **44**, 838-850 (1954).
20. Lyapustin, A., "Radiative transfer code SHARM-3D for radiance simulations over a non-Lambertian nonhomogeneous surface: intercomparison study," *Appl. Optics* **41**, 5607-5615 (2002).
21. Gatebe, C. K., M. D. King, A. I. Lyapustin, G. T. Arnold, and J. Redemann, "Airborne spectral measurements of ocean directional reflectance," *J. Atmos. Sci.* **62**, 1072-1092 (2005).
22. Nakajima, T., and M. Tanaka, "Algorithm for radiative intensity calculations in moderately thick atmospheres using a truncation approximation," *J. Quant. Spectrosc. Radiat. Transfer* **40**, 51-69 (1988).
23. Lyapustin, A., "Interpolation and Profile Correction (IPC) method for shortwave radiative transfer in spectral intervals of gaseous absorption," *J. Atmos. Sci.* **60**, 865-871 (2003).
24. Karp, A. H., J. Greenstadt, and J. A. Fillmore, "Radiative transfer through an arbitrarily thick, scattering atmosphere," *J. Quant. Spectrosc. Radiat. Transfer* **24**, 391-406 (1980).
25. Dave, J. V., "A direct solution of the spherical harmonics approximation to the radiative transfer equation for an arbitrary solar elevation," *J. Atmos. Sci.* **32**, 790-798 (1975).
26. S. Chandrasekhar, *Radiative Transfer*, Dover, New York (1960).
27. Lyapustin, A., Y. Wang, J. Martonchik, J. Privette, B. Holben, I. Slutsker, A. Sinyuk, and A. Smirnov, "Local Analysis of MISR Surface BRF and Albedo over GSFC and Mongu AERONET Sites," *IEEE Trans. Geosci. Remote Sens.*, submitted (2005).
28. Gao, F., X. Li, A. Strahler, and C. Schaaf, "Evaluation of the Li Transit kernel for BRF modeling," *Rem. Sens. Reviews* **19**, 205-224 (2000).
29. Hale, G. M., and M. R. Querry, "Optical constants of water in the 200-nm to 200  $\mu\text{m}$  wavelength region," *Appl. Optics* **12**, 555-563 (1973).
30. Gordon, H. R., and M. Wang, "Surface-roughness considerations for atmospheric correction of ocean color sensors. I: The Rayleigh-scattering component," *Appl. Optics* **31**, 4247-4260 (1992).

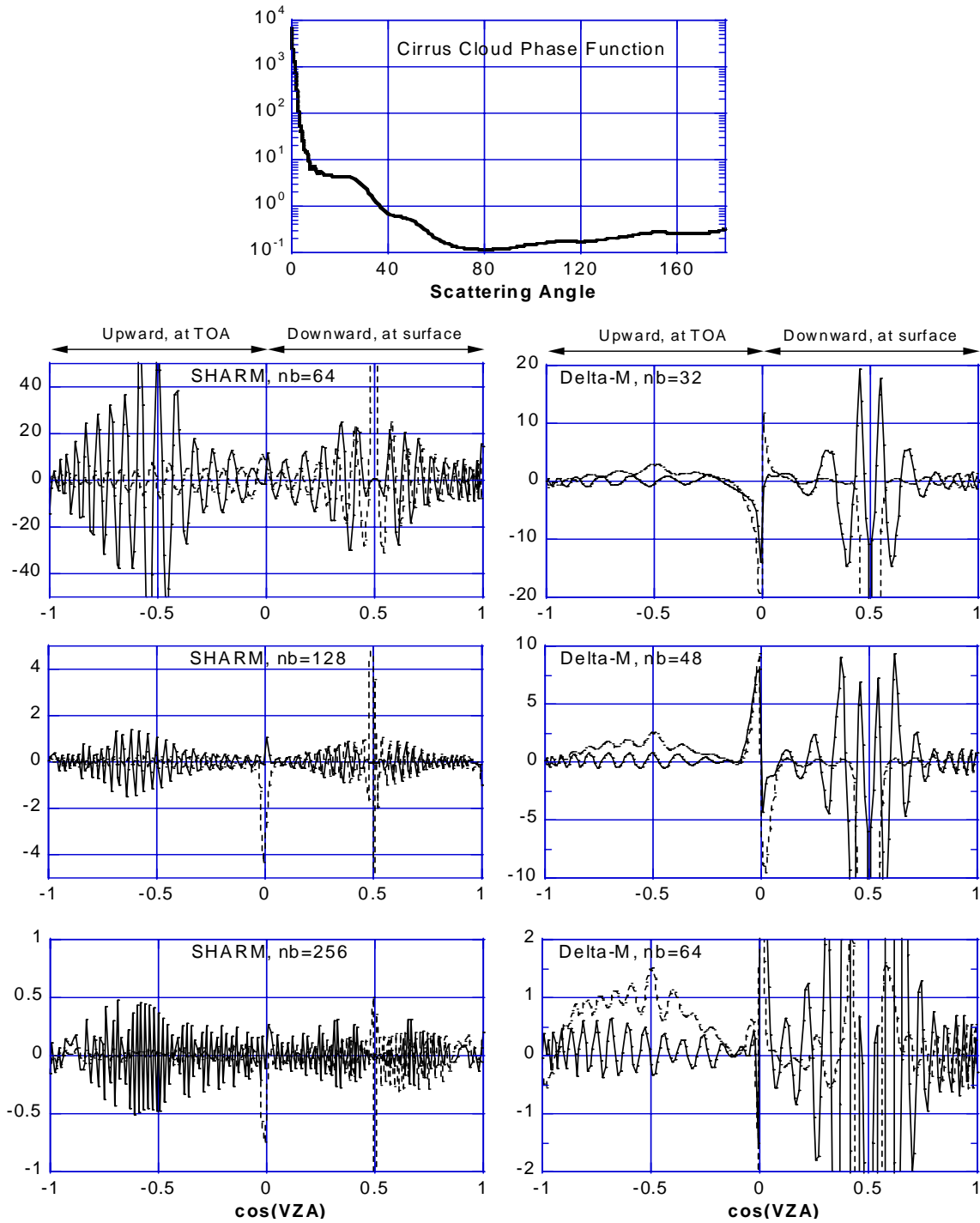


**Figure 1. Convergence of code SHARM (left) and SHARM with Delta-M method (right) for cirrus cloud.** The results are shown as a relative error (%) of SHARM radiance for different orders of MSH calculated with respect to the solution with  $nb=512$ . Calculations were performed for  $\tau=0.8$  and  $SZA=60^\circ$ . The solid and dashed lines represent the relative azimuth of  $0^\circ$  and  $180^\circ$  respectively. The negative and positive values on the abscissa axis relate to the upward radiance at the top of the atmosphere, and to the diffuse sky radiance incident on surface, respectively. The cirrus cloud phase function at  $\lambda=0.66 \mu\text{m}$  corresponds to  $10 \mu\text{m}$  ice particles.